Title

NON-EQUILIBRIUM FISSION AND HEAVY RESIDUE PRODUCTION IN THE INTERACTION OF 12-16 MEV/NUCLEON [SUP]32 S WITH [SUP]165 HO

Authors

Casey, C.
Loveland, W.
Xu, Z.

Publication Date

1988-09-01

LBL-25940
Preprint

Lawrence Berkeley Laboratory
UNIVERSITY OF CALIFORNIA

Submitted to Physical Review C

Non-Equilibrium Fission and Heavy Residue Production in the Interaction of 12–16 MeV/nucleon ^{32}S with ^{165}Ho

C. Casey, W. Loveland, Z. Xu, L. Sihver, K. Aleklett,
and G.T. Seaborg

September 1988

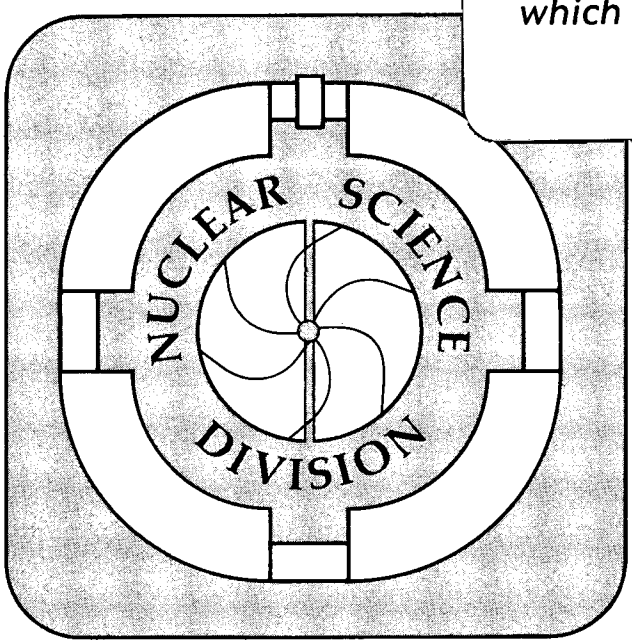

Prepared for the U.S. Department of Energy under Contract Number DE-AC03-76SF00098.

DISCLAIMER

Non-Equilibrium Fission and Heavy Residue Production in the Interaction of 12-16 MeV/nucleon ^{32}S with ^{165}Ho

C. Casey, W. Loveland, Z. Xu

Dept. of Chemistry

Oregon State University

Corvallis, OR 97331

L. Sihver, K. Aleklett

Studsvik Neutron Research Laboratory

S-611 82 Nykoping

Sweden

and

G.T. Seaborg

Nuclear Science Division

Lawrence Berkeley Laboratory

1 Cyclotron Road

Berkeley, CA 94720

September 1988

This work was supported by the Director, Office of Energy Research, Office of High Energy and Nuclear Physics, Nuclear Physics Division of the U.S. Department of Energy under Contract DE-AC03-76SF00098.

Non-Equilibrium Fission and Heavy Residue Production in the Interaction of 12-16 MeV/nucleon ^{32}S with ^{165}Ho

C. Casey, W. Loveland, Z. Xu

Dept. of Chemistry

Oregon State University

Corvallis, OR 97331

L. Sihver, K. Aleklett

Studsvik Neutron Research Laboratory

S-611 82 Nykoping

Sweden

and

G.T. Seaborg

Nuclear Science Division

Lawrence Berkeley Laboratory

Berkeley, CA 94720

Abstract:

The target fragment production cross sections, angular distributions, and range distributions have been measured for the interaction of 12-16 MeV/nucleon ^{32}S with ^{165}Ho. The fragment isobaric yield distribution and the fragment moving frame angular distributions have been deduced from the data. Symmetry properties of the moving frame angular distributions have been used to establish a relative time scale for the reaction mechanism(s). No fission fragment moving frame angular distribution is symmetric about 90°, suggesting that these products are predominantly produced by a fast, non-equilibrium process. The range distributions are used to deduce energy spectra, which suggest that the heavy residues are the result of complete or incomplete fusion and also of an inelastic process such as deep inelastic scattering.

PACS Numbers 25.70.Np

I. Introduction

Studies of intermediate energy nuclear collisions are thought to be interesting because of the "transitional" character of the intermediate energy regime. In low energy nuclear collisions, the behavior of the colliding nuclei is determined by their mean field while in high energy nuclear collisions, it is the collision of individual nucleons in the colliding nuclei that determines the outcome of the reaction. The intermediate energy regime (projectile energies of 10 to 100 MeV/nucleon) is thought to afford the opportunity of studying how nuclear reaction mechanisms change between these two extreme types of nuclear behavior.

The study of intermediate energy nuclear collisions has many aspects. In this discussion, we shall focus our attention on the experimental characterization of the fragments of the heavy target nucleus produced in such collisions. These fragments may be roughly classified by mass number, i.e., the intermediate mass fragments ($A_{frag} < A_{target}/3$); the heavy residues ($A_{frag} > (2/3)\ A_{target}$) and the fission fragments ($A_{target}/3 < A_{frag} < \frac{2}{3}\ A_{target}$). Interest in this area by experimentalists and theoreticians has been quite high, judging from the large number of survey papers and original contributions[1-30] that have appeared recently. From these many investigations, certain general features of the production of the target fragments have been discerned. They are:

1. The heavy residue production cross sections represent a significant fraction of the total reaction cross section.[5,7,12,23,24,27,29] The heavy residues are produced mostly in peripheral collisions at the higher projectile energies (35 and 44 MeV/nucleon)[18,23,30] although some residues at higher energies result from more central collisions as do

most residues at lower projectile energies[23,30] where they can be characterized as evaporation residues[27]. The heavy residue angular distributions are strongly forward-peaked in all cases[23,24,27]. Their velocities range from very low (at higher projectile energies where detector thresholds preclude observation of some residues[24,27]) to velocities exceeding that of the center of mass (indicating the existence of large nuclear excitation energies). Most of these fragments are produced in incomplete fusion reactions[11,12,18,23,30] although some are produced in nearly complete fusion events[23,30].

2. The intermediate mass fragment production cross sections are substantially lower than those of the heavy residues. They are predominantly produced with a multiplicity of unity in binary events that also yield a heavy residue[3,14,17,25,26]. The reactions producing them involve both non-equilibrated and equilibrated sources with the former being more important (in rections induced by carbon projectiles)[17,31,32]. Incomplete fusion with substantial pre-equilibrium particle emission is the dominant production mechanism.[14,17,26]

3. The fission fragments represent those primary heavy residue reaction products that deexcited by fission rather than particle emission[12,24,27] and also can represent the result of a special nuclear reaction mechanism, fast fission.[3,6,10,28] In the former case, one notes that $\frac{\tau_{HR}}{\tau_{fission}}$ increases with increasing projectile energy due to two effects (a) the increasing probability of incomplete fusion, leading to lower mass and atomic numbers of the product nuclei, thus decreasing their fissionability and (b) the faster time scale of the more energetic reactions favors the intrinsically faster process of particle emission

vs. the slower collective motion of fission.[27] Whether fission selects the high momentum transfer events relative to those of lower momentum transfer appears to be a complicated feature of the de-excitation of a given set of nuclei.

Recently Aleklett et al.[33] have studied the interaction of 17 MeV/nucleon ^{32}S, 32 MeV/nucleon ^{40}Ar and 44 MeV/nucleon ^{40}Ar with ^{197}Au. They observed a fast, non-equilibrium fission process associated with central collision events in these reactions. This observation motivated the present study in that we wanted to further characterize this non-equilibrium fission process. To do so, we studied the interaction of ~16 MeV/nucleon ^{32}S with a different nucleus, ^{165}Ho. By changing the target nucleus to ^{165}Ho, a nucleus that only fissions when made to rotate rapidly,[34] our hope was to observe the effects of a higher fission barrier, higher angular momentum of the fissioning system and a smaller change in deformation in going from saddle-to-scission upon this non-equilibrium fission mode. We were also aware of the existence of a large amount of data[35] for the interaction of intermediate energy, lighter projectiles, such as ^{12}C and ^{16}O, with ^{165}Ho.

II. Experimental Procedures

Inclusive measurements of the target fragment yields, angular distributions and differential range spectra for the interaction of 529 MeV ^{32}S with ^{165}Ho were made using radiochemical techniques. The accelerator used in the irradiations was the LBL 88" cyclotron. The measurements were made using techniques that have been described previously.[31,32,36,37] Two irradiations, of duration 1.25 and 6.53 hours, respectively, were performed to determine the target fragment yields (total fluences $2.4X10^{15}$ and $6.7X10^{16}$ ions, respectively). The targets for these irradiations were ~90mg/cm^2 thick,

giving[38] a center-of-target energy of ~380 MeV (~12 MeV/nucleon). Two irradiations were used for the angular and range distribution measurements of 16.2 and 14.2 hours with particle fluences of $2.9X10^{15}$ and $5.4X10^{15}$ particles, respectively. Because of the thinner targets involved (152νg/cm^2 Ho deposits on a 2.95 mg/cm^2 Be backing), the center of target energies were 508 MeV (16 MeV nucleon).

III. Results

For the reaction of 12-16 MeV ^{32}S with ^{165}Ho, partial and complete angular distributions of 82 different target fragments were measured along with the production cross sections for 75 different radionuclides. Differential range distributions were obtained for 31 radionuclides.

A. Target Fragment Yields

The measured target fragment production cross sections are shown in Table I. We have taken a conservative approach in this tabulation and have eliminated from the table all references to all nuclides whose atomic and mass numbers are such that they could possibly be degraded projectile fragments. In doing so, we have effectively eliminated intermediate mass fragments from our study. We have deduced mass yield (isobaric yield) distributions from the measured formation cross sections. The method employed in this estimation procedure has been discussed previously.[36]

The measured nuclidic formation cross sections were placed in eight groups according to mass number. These cross sections were corrected for precursor beta decay, where necessary, by assuming that the independent yield cross sections for a given species, $\tau(Z,A)$, can be expressed as a histogram that lies along a Gaussian curve.

$$\tau(Z,A) = \tau(A)[2\pi C_Z^2(A)]^{-1/2} \exp[\frac{-(Z-Z_{mp})^2}{2C_Z^2(A)}] \quad (1)$$

where $C_Z(A)$ is the Gaussian width parameter width parameter for mass number A and $Z_{mp}(A)$ is the most probable atomic number for that A. Using this assumption and the further assumption that $\tau(a)$ varies slowly and smoothly as a function of A (allowing data from adjacent isobars to be combined in determining $Z_{mp}(A)$ and $C_Z(A)$), one can use the laws of radioactive decay to iteratively correct the measured cumulative formation cross sections for precursor decay.

Within each of the eight groups, the data were fit to a Gaussian-shaped independent yield distribution. The width parameter was found to be constant over a given range in A while the centers of the charge distributions were adequately represented by linear functions in A over a limited range in A although we expect $Z_{mp}(A)$ to be non-linear. (Only nuclides with well-characterized beta-decay precursors and cases where both members of an isomeric pair were observed were included in the analysis). The nuclidic groupings along with the centers and widths of the Gaussian distributions are given in Table II. The independent yield distributions estimated from the measured formation cross sections are shown in Figure 1.

The isobaric yield distribution obtained from integration of the estimated independent yield distributions is shown in Figure 2. The error bars on the integrated data points reflect the uncertainties due to counting statistics and those introduced in the charge distribution fitting process. Morrissey *et al.*[36] have suggested that individual isobaric yields may have systematic uncertainties, due to the fitting process, of approximately 25%. Uncertainties due to lack of knowledge of the absolute beam intensity

(estimated to be approximately 15%), and contributions due to secondary reactions (possibly as large as 10%) have been neglected. Also shown as smooth curves in Figure 2 are the isobaric yield distributions for the interaction[35] of roughly equivalent velocity ^{16}O ions with ^{165}Ho. (normalized to the $^{32}S + ^{165}Ho$ total reaction cross section[39]) as well as roughly equivalent total projectile energy ^{12}C with ^{165}Ho.

One notes two prominent peaks in the isobaric distributions, a fission peak (A=50-146) and a heavy residue peak (A>146). The fission cross section is enhanced for the $^{32}S + ^{165}Ho$ reaction relative to the other reactions (τ_f = 2060mb) with especially higher yields of the heavy mass fission products. The latter observation is consistent with the larger A value of the completely fused system in the $^{32}S + ^{165}Ho$ reaction.

The relative fission cross section in these reactions can be understood in terms of a correlation[34] between the relative fission cross section and the angular momentum transferred to the target nucleus (Figure 3). The data from the $^{32}S + ^{165}Ho$ appears to fit well into the previously established correlation.

B. Target Fragment Angular Distributions

Full or partial angular distributions for 82 different target fragments were measured. Discussion of corrections due fragment scattering, finite beam spot size, etc. is presented elsewhere[40]. A representative set of these distributions is shown in Figure 4. The laboratory frame angular distributions are all strongly forward-peaked. The heavy residue angular distributions (A > 146) have different shapes than those associated with fission products that are consistent with relative momentum kicks given the primary fragments by fission or sequential particle emission.

Each fragment angular distribution was integrated from 0 to $\Pi/2$ and $\Pi/2$ to Π to obtain the ratio of fragments recoiling forward (F) from the target to those recoiling backward (B). To extract further information from the data, the laboratory system angular distributions were transformed into the moving frame of the target residue following the initial target-projectile encounter. To do this, we have assumed that the final velocity of the fragment in the laboratory system can be written as $V_{lab} = V + v$, where the velocity v is the velocity of the moving frame and V is the velocity kick given the target fragment by particle emission or fission at an angle Ψ_{MF} with respect to the beam direction in the moving frame. The vector v has components of v_{11} and $v_{\perp}$, parallel and perpendicular to the beam direction. In lieu of detailed information about $v_{\perp}$, the forward-peaked nature of the distributions and the difficulty of obtaining information about $v_{\perp}$, we have assumed $v_{\perp} = 0$. We have used standard formulas[41] to make laboratory frame transformations for $d\sigma/d\Omega$ and Ψ.

For the value of θ_{11} ($=v_{11}/V$) needed to make such transformations, we have used θ_{11} as derived from integrating the angular distributions, where θ_{11} = (F-B)/(F+B). Previous work[33] has shown that values of θ_{11} deduced in this manner agree with directly measured values. A representative set of the resulting moving frame angular distributions for the fission fragments is shown in Figure 5. (Not enough data was available at backward angles to meaningfully transform the heavy residue distributions). None of the moving frame angular distributions is symmetric about 90° in the moving frame (Fig. 6). This unique observation suggests the occurrence of a fast, non-equilibrium mode of fission (similar to that previously observed[33] for the reaction of 17-44 MeV/nucleon ^{32}S and ^{40}Ar with ^{197}Au). However, unlike the

^{32}S, ^{40}Ar + ^{197}Au reactions where this mechanism was only discernible in the angular distribution of the heavy mass fission fragments, the occurrence of this mechanism is clearly seen for all fission fragments although it is most prevalent for the high mass number fragments (Fig. 6.)

C. Target Fragment Energy Spectra

The measured differential range spectra were converted to energy spectra using standard range-energy tables.[42] A representative set of these data is shown (in Fig. 7). The energies of the fission fragments are consistent with what is expected for the fission of composite nuclei following the complete fusion of 16 MeV/nucleon ^{32}S with ^{165}Ho. The ^{160}Er spectrum is typical of those spectra for fragments with A = 140 - 165, showing peaks in the energy spectra at ~0.1 Mev/A and 0.5 MeV/A.

IV. Discussion of Results

A. Heavy Residues

At projectile energies of 12-16 MeV/nucleon, one would expect that about 15-25% of the reactions involved complete fusion[39]. The success of the Boltzmann master equation model of Blann[43] in accounting for many features of intermediate energy heavy ion reactions would suggest that a substantial fraction of the reactions would involve pre-equilibrium emission. We have used the computer program LINDA[44] to simulate the production of the heavy residues assuming production via: (a) complete fusion or (b) pre-equilibrium emission as predicted by the Blann pre-equilibrium emission model. (For this reaction, 2 protons and 5 neutrons were predicted to be emitted prior to the establishment of equilibrium).

The results of the simulations are compared to the experimental data for a typical heavy residue, ^{170}Hf, in figure 8. The predicted differences

between the two reaction mechanisms are barely discernible. The resolution of the measured data does not allow one to determine which mechanism is dominant but the data agrees well with either prediction.

As noted previously, in addition to the main peak in the heavy residue energy spectra at ~0.5 MeV/nucleon due to complete or incomplete fusion, there is another peak at ~0.09 MeV/nucleon. Such energies are consistent with the production of these fragments in deep inelastic events where Q ~-200 MeV. The resulting damped projectile-like fragments (A~30) would have energies ~10-11 MeV/nucleon which is consistent with the range spectra of fragments such as ^{28}Mg.

B. Fission Products

None of the fission products had moving frame angular distributions which were symmetric about 90°. This fact suggests the production, in part, of these fragments by a fast, non-equilibrium mechanism. Production of these fragments by a normal, "slow" fission process would be expected to occur also and a modest contribution of non-equilibrium fission events to the total fission fragment angular distributions would cause them to be asymmetric. (In this context, "slow" and "fast" are defined relative to the time estimated[45] for the establishment of statistical equilibrium in an excited nuclear system of $2\text{-}3X10^{-23}$ sec).

A known nuclear reaction mechanism for low energy nucleus-nucleus collisions, "fast fission" or "quasifission"[28] would appear to be a possible candidate for the suggested non-equilibrium mechanism. In this mechanism, all partial waves between the l-wave at which the fission barrier vanishes, $l_{B_f}=0$ and the critical angular momentum, l_{crit}, go via fast fission. In these events, the fusing system never reaches a configuration inside the fission saddle point and the resulting fission event is fast. Experimental signatures

for such events are the lack of symmetry of the angular distributions in the moving frame and a broader than normal fission mass distribution (Figure 2). Unlike the previous studies[33] of the intermediate energy ^{32}S, ^{40}Ar + ^{197}Au reactions where it was possible to resolve the fragment angular distributions into "slow" and "fast" components, the lack of any distribution being symmetric in the moving frame precludes such a decomposition. As a first guess at an alternate decomposition, if one assumes the slow equilibrium component of the fission cross section to be ~1620mb (as observed in the 17 MeV/nucleon ^{16}O + ^{165}Ho reaction where $l_{Bf=0} > l_{crit}$) then one obtains, by difference, an estimated non-equilibrium cross section of ~440mb, which is twice the expected fast fission cross section. A similar effect was observed by Aleklett et al.[33] for the reaction of 17 A MeV ^{32}S with ^{197}Au where the non-equilibrium fission cross section was estimated to be ~2.9X the fast fission cross section.

The measured fission cross section for the 12 Mev/nucleon ^{32}S + ^{165}Ho reaction seems to fit in well with a previously established empirical correlation[34] between the fraction of primary residues that fission and a semiclassical estimate of the angular momentum transferred to the target nucleus. We attempted to see if this apparent empirical correlation observed for the interaction of ^{12}C, ^{16}O and ^{32}S nuclei with ^{165}Ho would be expected from standard statistical model calculations of the de-excitation of highly excited nuclei. As our "standard statistical model" we used the PACE code,[46] an angular momentum dependent Monte Carlo model. For projectile energies below 10 MeV/nucleon, we simply treated the problem as a compound nucleus formation and decay problem. The fusion cross sections were adjusted to published systematics of experimental data.[39] The ratio of level density

parameters a_f/a_n was taken to be 1.000. The finite range rotating liquid drop fission barriers of Sierk[47] were used in the calculation. For projectile energies above 10 MeV/nucleon, the distribution of (E*,J,Z,A) of the target fragments following the primary nucleus-nucleus collision was calculated using the Boltzmann Master equation model as described previously.[48] The results of these simulations are shown in figure 3. Although there are some differences between the calculated and measured fission probabilities in each system, the calculations generally reproduce the data. While the fission probabilities shown in Figure 3 reflect both the effects of E* and J of the fissioning system, the primary effect (in the statistical model) is one due to the J of the fissioning system.

V. Conclusions

What new information have we gained about intermediate energy nucleus-nucleus collisions from this study? The use of radiochemical techniques for measuring energy spectra and the use of very thin targets has allowed us to measure the heavy residue energy spectra down to very low energies. These measurements seem to indicate the occurrence of deep inelastic scattering as a heavy residue production mechanism (in the interaction of 16 MeV/nucleon ^{32}S with ^{165}Ho).

The fission fragment mass distribution observed in this work is substantially broader than that observed in the interaction of equivalent velocity or total projectile kinetic energy ^{12}C and ^{16}O projectiles with ^{165}Ho. The angular distributions show the importance of fast, non-equilibrium fission processes. The relative dominance of these processes when ^{165}Ho is the target nucleus compared to ^{197}Au could be due to the larger fraction of fission events taking place at high angular momentum. The previously

established empirical correlation between fission probability and semi-classical measure of the transferred angular momentum in the reaction has been shown to be consistent with a standard statistical model for the de-excitation of hot rotating nuclei.

Acknowledgements

We wish to thank Ruth Mary Larimer and the crew of the 88" cyclotron for their help as well as Diana Lee of LBL for assistance during counting of samples. Helpful discussions with T.T. Sugihara are gratefully acknowledged. This work was supported in part by the U.S. Dept. of Energy through Grant No. DE-FG06-88ER40402.

This work was supported by the Director, Office of Energy Research, Office of High Energy and Nuclear Physics, Nuclear Physics Division of the U.S. Department of Energy under Contract DE-AC03-76SF00098.

Table I
Formation cross sections (mb) of nuclides formed by the reaction of 12 MeV/nucleon ^{32}S with ^{165}Ho.
Independent yields are indicated by (I)*.

NUCLIDE		CROSS SECTION		
^{42}K		9.8	±	0.5
^{43}K		11.2	±	0.3
^{46}Sc	(I)	11.5	±	0.5
^{47}Ca		1.60	±	0.06
^{48}Sc	(I)	5.2	±	0.6
^{48}V		2.26	±	0.03
^{52}Mn		1.50	±	0.01
^{56}Mn		18.	±	2.
^{592}Fe		10.0	±	0.3
^{65}Zn		15.	±	1.
^{69}Ge		11.2	±	0.9
^{73}Se		4.2	±	0.1
^{74}As	(I)	30.	±	2.
^{75}Se		29.4	±	0.9
^{75}Br		2.5	±	0.2
^{76}Br		14.	±	6.
^{77}Br		32.	±	2.
^{79}Kr		21	±	10.
^{81}Rb		18.1	±	0.9
^{82}Br	(I)	5.8	±	0.4
$^{82}Rb^{m}$		28	±	4.
^{83}Rb		56.	±	4.
^{84}Rb	(I)	39	±	1.
^{86}Y		28	±	2.
^{87}Y		62.3	±	0.9
^{88}Y		40.	±	2.
^{88}Zr		36.	±	2.
^{89}Zr		51.	±	1.
^{90}Nb		25.	±	2.
$^{92}Nb^{m}$	(I)	1.6	±	0.5
^{93}Tc		3.3	±	0.3
^{94}Tc		10.	±	2.
^{95}Ru		3.1	±	0.2
^{95}Tc		18.	±	3.
^{96}Tc	(I)	30.6	±	0.2
^{97}Ru		18.1	±	0.7
^{100}Rh		23.6	±	0.4
$^{101}Rh^{m}$		33.	±	1.0
^{105}Ag		33.	±	5.
^{111}In		30.6	±	0.7
^{123}I		36.	±	1.
^{123}Xe		15.9	±	0.8
^{124}I		3.8	±	0.2
^{126}Ba		7.7	±	0.9
^{127}Cs		14.3	±	0.5
^{127}Xe		15.	±	6.
^{128}Ba		25.	±	8.
^{129}Cs		20.2	±	0.8
^{132}Ce		10.0	±	0.6
^{135}Ce		16.	±	2
^{139}Ce		6.	±	1.
^{145}Eu		11.2	±	0.3
^{146}Eu		7.4	±	0.4
^{149}Gd		24.	±	1.
^{151}Tb		18.	±	3.
^{152}Tb		15.	±	2.
^{153}Tb		27.	±	2.
^{155}Tb		37.	±	11.
^{155}Dy		31.3	±	0.7
^{156}Tb	(I)	5.5	±	0.2
^{157}Dy		48.7	±	0.9
^{160}Er		94.	±	6.
^{161}Er		82.	±	3.
^{163}Tm		94.	±	22.
^{165}Tm		156.	±	23.
^{166}Yb		54.	±	5.
^{167}Tm		76.	±	4.
^{169}Lu		29	±	1.
^{170}Hf		16.9	±	0.8
^{171}Hf		14.	±	1.0
^{173}Hf		12.7	±	0.4
^{173}Ta		4.	±	2.
^{175}Hf		22.	±	1.

*By the term "independent yield", we refer to the yields of shielded nuclides, quasi-shielded nuclides and nuclides whose production by precursor decay is not significant.

Table II
Charge Dispersion Parameters

Fragment Mass Number Range	$Z_{mp}(A)$	$C_Z(A)$
42-49	0.433A + 1.07	0.7
65-79	0.438A + 0.76	0.7
81-89	0.441A + 0.37	0.7
90-100	0.439A + 0.70	0.8
101-124	0.384A - 6.20	0.9
126-139	0.373A - 7.85	0.9
145-160	0.375A - 7.63	0.7
161-175	0.362A + 9.76	0.3

References

1 S. Levit in Proc. Int'l Nucl. Phlys. Conf. Harrogate, J.L. Durell, J.M. Irvine, and G.C. Morrison, ed. (Institute of Physics, Bristol. 1987) p. 227.

2. M. Conjeaud, S. Harar, M. Mostefai, E.C. Pollaco, C. Volant, Y. Cassagnou, R. Dayras, R. Legrain, H. Oeschler, and F. Saint-Laurent, Phys. Lett. 159B, 244 (1985).

3. S. Harar, Nucl. Phys. A471, 205c (1987).

4. B. Tamain, in Proc. Int'l Nucl. Phys. Conf., Harrogate, J.L. Durell, J.M. Irvine, and G.C. Morrison, ed. (Institute of Physics, Bristol, 1987) p. 247.

5. F. Hubert, R. Del Moral, J.P. Dufour, H. Emmermann, A. Fleury, C. Poinot, M.S. Pravikoff, H. Delagrange, and A. Lleres, Nucl. Phys. A456, 535 (1986).

6. H. Delagrange, C. Gregoire, Y. Abe, and N. Carjan, J de Physique, 47, C4-305 (1986).

7. J. Blachot, J. Crancon, B. deGoncourt, A. Gizon, and A. Lleres, Z. Phys., A321, 645 (1985).

8. H. Nifenecker, J. Blachot, J. Crancon, A. Gizon, and A. Lleres, Nucl. Phys., A447, 533c (1985).

9. D. Jacquet, E. Duek, J.M. Alexander, B. Borderie, J. Galin, D. Gardes, D. Guerreau, M. Lefort, F. Monnet, M.F. Rivet, and X. Tarrago, Phys. Rev. Lett. 53, 2226 (1984).

10. W.P. Zank, D. Hilscher, G. Ingold, U. Jahnke, M. Lehmann, and H. Rossner, Phys. Rev. C33, 519 (1986).

11. D. Guerreau, Nucl. Phys. A4447, 37c (1985).

12. C. Cerruti, D. Guinet, S. Chiodelli, A. Demeyer, K. Zaid, S. Leray, P. Lhenoret, C. Mazur, C. Ngo, M. Ribrag, and A. Lleres, Nucl. Phys. A453, 175 (1986).

13. Y. Patin, S. Leray, E. Tomasi, O. Granier, C. Cerruti, J.L. Charvet, S. Chiodelli, A. Demeyer, D. Guinet, C. Humeau, P. Lhenoret, J.P. Lochard, R. Lucas, C. Mazur, M. Morjean, C. Ngo, A. Pehaire, M. Ribrag, L. Sinopoli, T. Suomijarvi, J. Uzureau, and L. Vagneron, Nucl. Phys. A457, 146 (1986).

14. K. Kwiatkowski, Nucl. Phys. A471, 271c (1987).

15. See, for example, J. Pochodzalla, Nucl. Phys. A471, 289c (1987); W.G. Lynch, ibid, 309c; D. Gross and H. Massman, ibid, 339c; J.P. Bondorf, et al., Nucl. Phys. A444, 460 (1985).

16. C. Gregoire, D. Jacquet, M. Pi, B. Remaud, F. Sebille, E. Suraud, P. Schuck, and L. Vinet, Nucl. Phys. A471, 399c (1987).

17. V.E. Viola, ibid, 53c.

18. H. Delagrange and J. Peter, ibid, 111c.

19. D. Fabris, K. Hagel, J.B. Natowitz, G. Nebbia, R. Wada, R. Billerey, B. Cheynis, A. Demeyer, D. Drain, D. Guinet, C. Pastor, L. Vagneron, T. Zaid, J. Alarja, A. Giorni, D. Heuer, C. Morand, B. Viano, C. Mazur, C. Ngo, S. Leray, R. Lucas, M. Ribrag, and E. Tomasi, ibid, 351c.

20. G. Auger, E. Plagnol, D. Jouan, C. Guet, d. Heuer, M. Maurel, H. Nifenecker, C. Ristori, F. Schussler, H. Doubre, and C. Gregoire, Phys. Lett. 169B, 161 (1986).

21. S. Leray, J. de Physique, 47, C4-273 (1986).

22. A. Lleres, C. Guet, D. Heuer, M. Maurel, C. Ristori, F. Schussler, M.W. Curtain and D.K. Scott, Phys. Lett. B185, 336 (1987).

23. G. Bizard, R. Brou, H. Doubre, A. Drouet, F. Guilbault, F. Hanappe, J.M. Harasse, J.L. Laville, C. Lebrun, A. Oubahadou, J.P. Patry, J. Peter, G. Ployart, J.C. Steckmayer and B. Tamain, Z. Phys. A323, 459 (1986).

24. G. Bizard R. Brou, H. Doubre, A. Drouet, F. Guilbault, F. Hannappe, J.M. Harasse, J.L. Laville, C. Lebrun, A. Oubahadou, J.P. Patry, J. Peter, G. Ployart, J.C. Steckmayer, and B. Tamain, Nucl. Phys. A456, 173 (1986).

25. B. Borderie, C. Cabot, H. Fuchs, D. Gardes, H. Gauvin, F. Hannappe, D. Jacquet, D. Jouan, F. Monnet, M. Montoya, and M.F. Rivet, Nouvelles de GANIL, NO. 22 (1987).

26. D.J. Fields, W.G. Lynch, T.K. Nayak, M.B. Tsang, C.B. Chitwood, C.K. Gelbke, R. Morse, J. Wilczynski, T.C. Awes, R.L. Ferguson, F. Plasil, F.E. Obenshain, and G.R. Young, Phys. Rev. C34, 536 (1986).

27. M.F. Rivet, B. Borderie, H. Gauvin, D. Gardes, C. Cabot, F. Hannappe and J. Peters, Phys. Rev. C34, 1282 (1986).

28. C. Gregoire, C. Ngo, and B. Remaud, Nucl. Phys. A383, 392 (1982).

29. E.C. Pollacco, M. Conjeaud, S. Harar, C. Volant, Y. Cassagnou, R. Dayras, R. Legrain, M.S. Nguyen, H. Oeschler, and F. Saint-Laurent, Phys. Lett. 146B, 29 (1984).

30 Y. Patin et al., Nucl. Phys. A457, 146 (1986).

31. R.H. Kraus, Jr., W. Loveland, K. Aleklett, P.L. McGaughey, T.T. Sugihara, G.T. Seaborg, T. Lund, Y. Morita, E. Hagebo, and I.R. Haldersen, Nucl. Phys. A432, 525 (1985).

32. K. Aleklett, W. Loveland, T. Lund, P.L. McGaughey, Y. Morita, G.T. Seaborg, E. Hagebo, and I. Haldorsen, Phys. Rev. C33, 885 (1986).

33. K. Aleklett, W. Loveland, L. Sihver, Z. Xu, C. Casey, D.J. Morrissey, J.O. Liljenzin, M. de Saint-Simon, and G.T. Seaborg, Nucl. Phys. A. (submitted for publication).

34. W. Loveland, K. Aleklett and G.T. Seaborg, Nucl. Phys. A447, 101c (1985).

35. R. Krause, Ph.D. thesis, Oregon State University, 1986 (unpublished).

36. D.J. Morrissey, W. Loveland, M. de Saint-Simon and G.T. Seaborg, Phys. Rev. C21, 1783 (1980).

37. D.J. Morrissey, D. Lee, R.J. Otto, and G.T. Seaborg, Nucl. Instr. Meth. 158, 499 (1978).

38. F. Hubert, A. Fleury, R. Bimbot, and D. Gardes, Ann. Phys. Fr. 5, 3 (1980).

39. W.W. Wilcke, J.R. Birkelund, H.J. Wollersheim, A.D. Hoover, J.R. Huizenga, W.U. Schroder and L.E. Tubbs, At. Data and Nucl. Data Tables 25, 391 (1980).

40. C. Casey, M.S. thesis, Oregon State University, 1988 (unpublished)

41. J.B. Marion, T.I. Arnette and H.C. Owens, Oak Ridge National Laboratory Report ORNL-2574, 1959.

42. L.G. Northcliffe and R.S. Schilling, Nucl. Data Tables 7, 233 (1970).

43. M. Blann, Phys. Rev. C31, 1245 (1985).

44. E. Duek, L. Kowalski and J.M. Alexander, Com. Phys. Comm. 34, 395 (1985).

45. G.D. Harp, J.M. Miller and B.J. Berne, Phys. Rev. 165, 1166 (1968).

46. A. Gavron, Phys. Rev. C21, 230 (1980).

47. A.J. Sierk, Phys. Rev. C33, 2039 (1986).

48. A.N. Behkami, W. Loveland, K. Aleklett and G.T. Seaborg, in Nuclear Fission and Heavy-Ion-Induced Reactions, W.U. Schroder, Ed. (Harwood, Loudon, 1987) pp. 443-451.

Figure Captions

Figure 1. The independent yield distributions from the reaction of 12 MeV/nucleon ^{32}S with ^{165}Ho. The plotted points are the independent yield cross sections calculated from the data while the solid lines are the Gaussian charge dispersions used in the calculation.

Figure 2. Isobaric yield distributions for the fragmentation of ^{165}Ho by (a) 12 meV/nucleon ^{32}S, solid points, solid line (b) 17 MeV/nucleon ^{16}O (ref. 35), dotted line (c) 442 MeV ^{12}C (ref. 35), dashed line.

Figure 3. Empirical systematics relating the fission probability to a semiclassical measure of the transferred angular momentum in the reaction.[34] The solid points refer to the interaction of ^{12}C and ^{16}O with ^{165}Ho, the open point ^{32}S + ^{165}Ho (this work) and the solid line represents the result of a calculation using a statistical model for the de-excitation of hot, rotating nuclei.

Figure 4. Representative laboratory frame fragment angular distributions for the interaction of 16 MeV/nucleon ^{32}S with ^{165}Ho.

Figure 5. Moving frame angular distributions derived from the data of figure 4.

Figure 6. The forward-to-backward ratios (F/B) vs. product mass number for the distributions shown in Figure 5.

Figure 7. Representative fragment energy spectra for the interction of 16 MeV/nucleon ^{32}S with ^{165}Ho.

Figure 8. Comparison of the predicted heavy residue angular distributions and energy spectra for an A=170 fragment with the observed ^{170}Hf data.

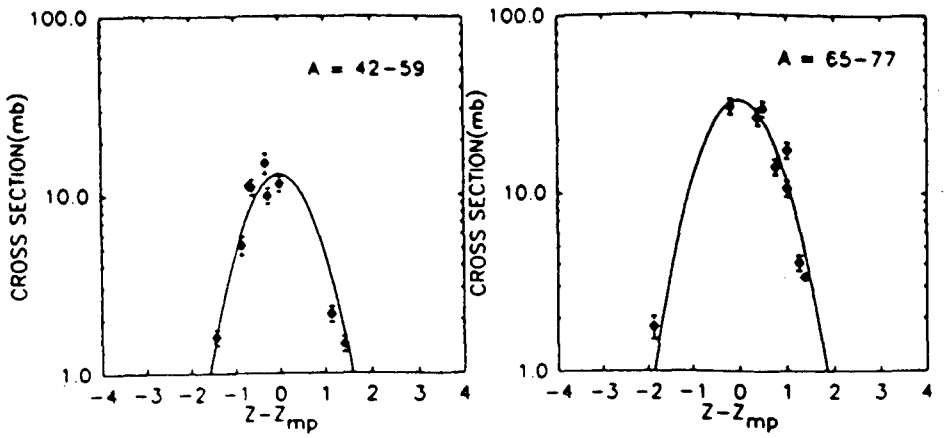
A = 42-59
CROSS SECTION(mb)
100.0
10.0
1.0
-4 -3 -2 -1 0 1 2 3 4
Z-Zmp

A = 65-77
CROSS SECTION(mb)
100.0
10.0
1.0
-4 -3 -2 -1 0 1 2 3 4
Z-Zmp

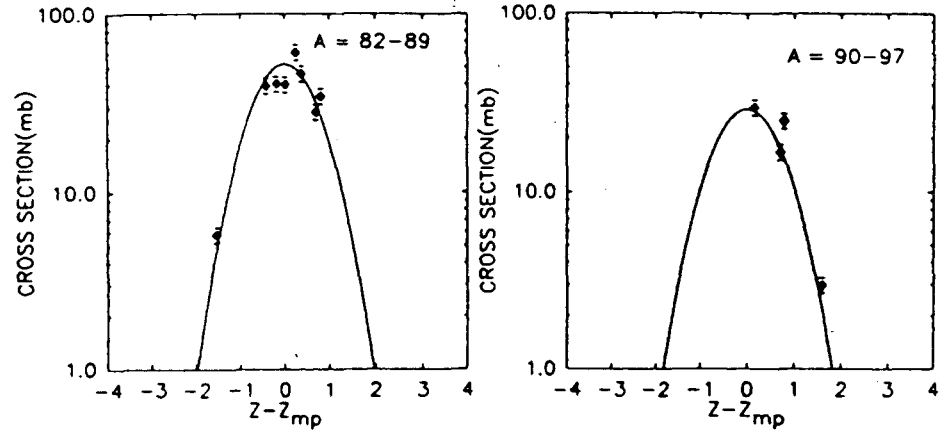
A = 82-89
CROSS SECTION(mb)
100.0
10.0
1.0
-4 -3 -2 -1 0 1 2 3 4
Z-Zmp

A = 90-97
CROSS SECTION(mb)
100.0
10.0
1.0
-4 -3 -2 -1 0 1 2 3 4
Z-Zmp

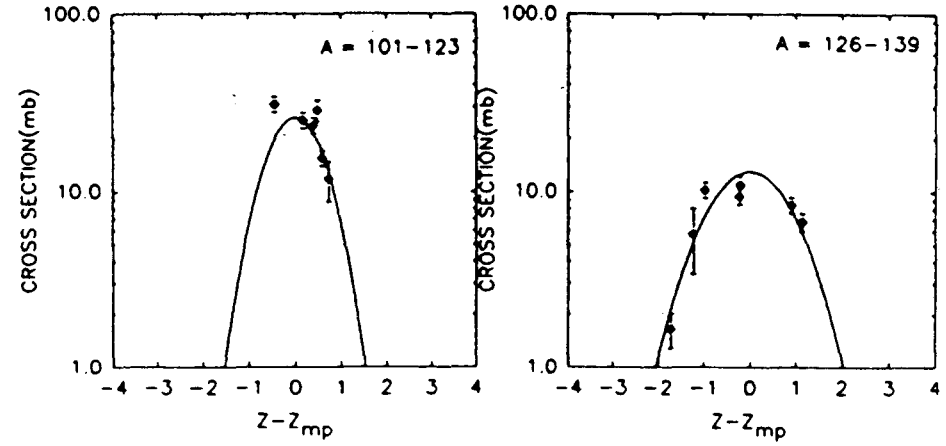
A = 101-123
CROSS SECTION(mb)
100.0
10.0
1.0
-4 -3 -2 -1 0 1 2 3 4
Z-Zmp

A = 126-139
CROSS SECTION(mb)
100.0
10.0
1.0
-4 -3 -2 -1 0 1 2 3 4
Z-Zmp

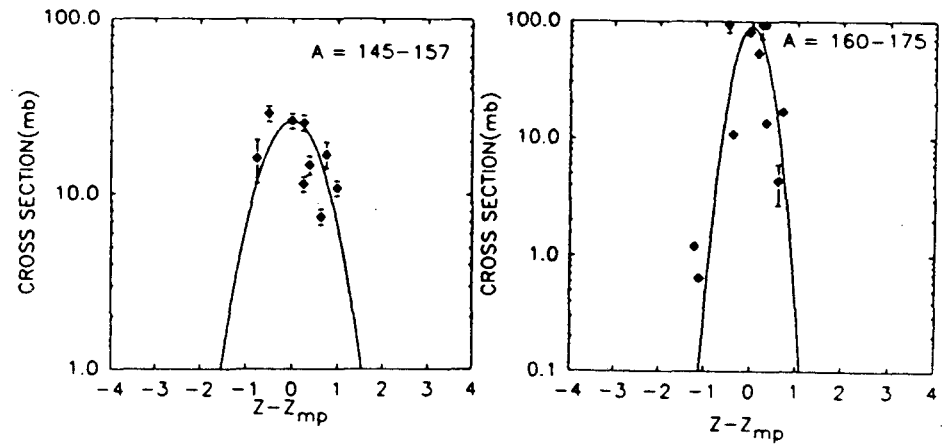
A = 145-157
CROSS SECTION(mb)
100.0
10.0
1.0
-4 -3 -2 -1 0 1 2 3 4
Z-Zmp

A = 160-175
CROSS SECTION(mb)
100.0
10.0
1.0
0.1
-4 -3 -2 -1 0 1 2 3 4
Z-Zmp

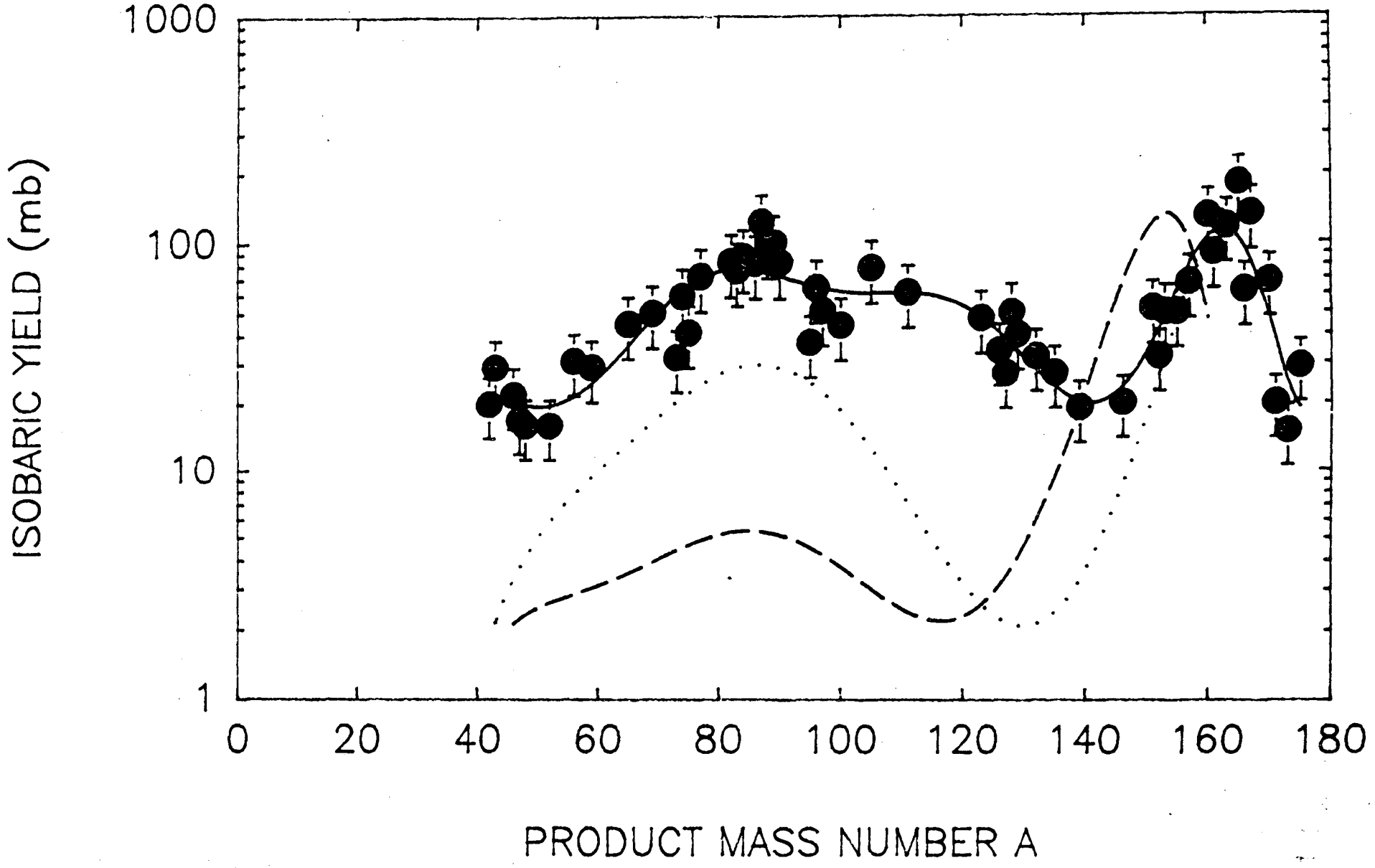
1000
100
10
1
ISOBARIC YIELD (mb)
0
20
40
60
80
100
120
140
160
180
PRODUCT MASS NUMBER A

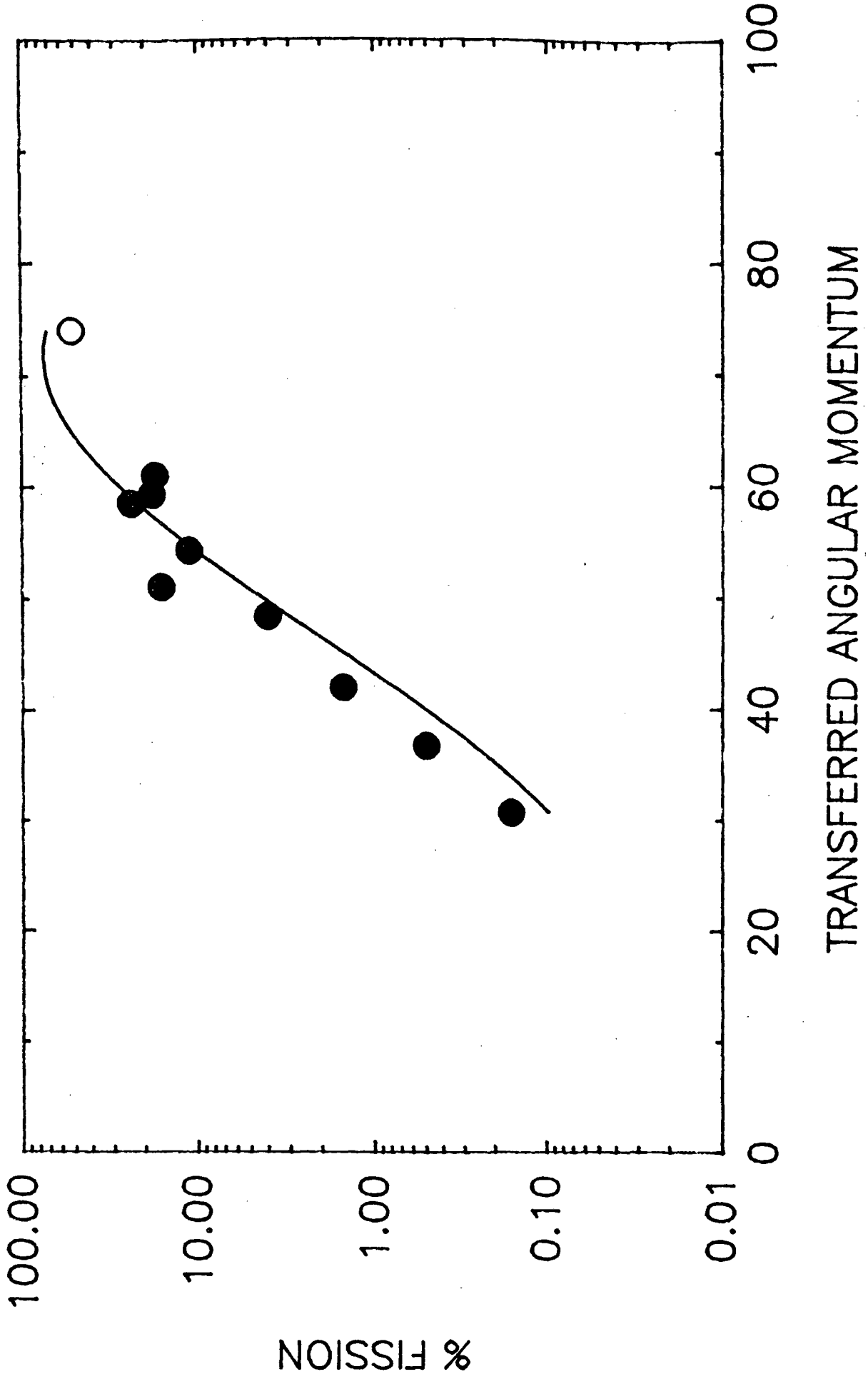
100.00
10.00
1.00
0.10
0.01
% FISSION
0
20
40
60
80
100
TRANSFERRED ANGULAR MOMENTUM

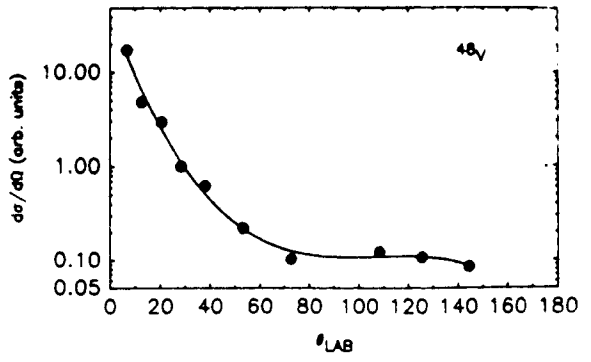
^{48}V
dσ/dΩ (arb. units)
10.00
1.00
0.10
0.05
0 20 40 60 80 100 120 140 160 180
θ_{LAB}

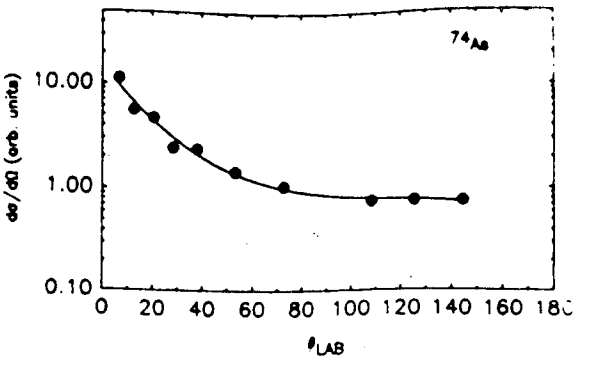
^{74}As
dσ/dΩ (arb. units)
10.00
1.00
0.10
0 20 40 60 80 100 120 140 160 180
θ_{LAB}

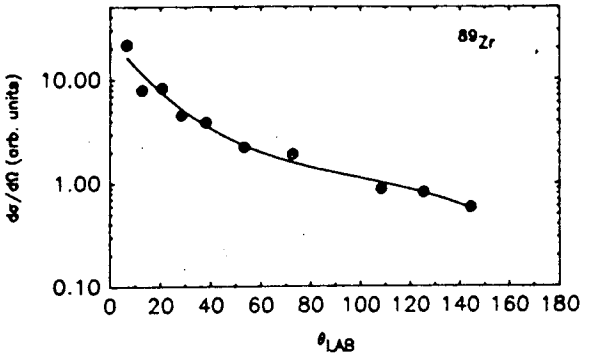
^{89}Zr
dσ/dΩ (arb. units)
10.00
1.00
0.10
0 20 40 60 80 100 120 140 160 180
θ_{LAB}

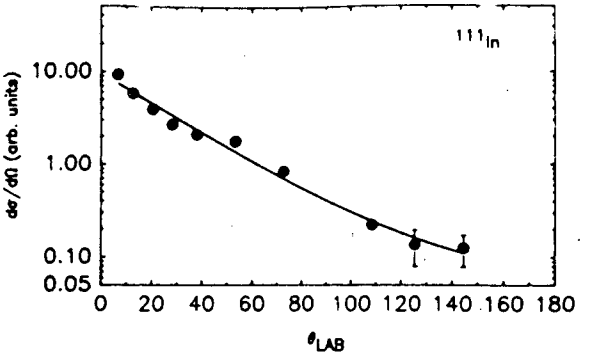
^{111}In
dσ/dΩ (arb. units)
10.00
1.00
0.10
0.05
0 20 40 60 80 100 120 140 160 180
θ_{LAB}

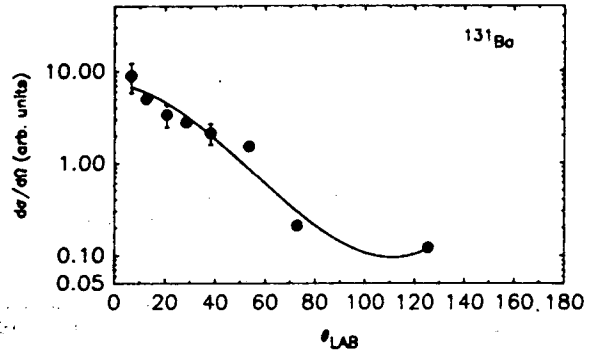
^{131}Ba
dσ/dΩ (arb. units)
10.00
1.00
0.10
0.05
0 20 40 60 80 100 120 140 160 180
θ_{LAB}

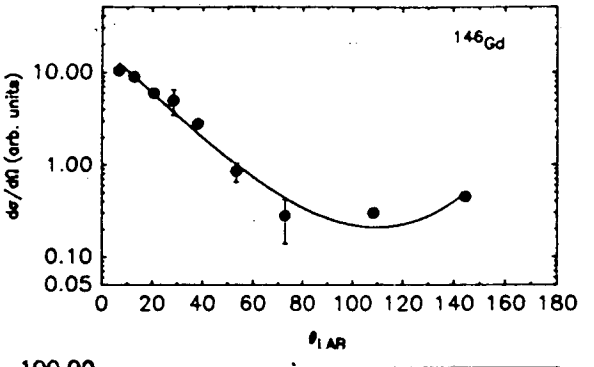
^{146}Gd
dσ/dΩ (arb. units)
10.00
1.00
0.10
0.05
0 20 40 60 80 100 120 140 160 180
θ_{LAB}

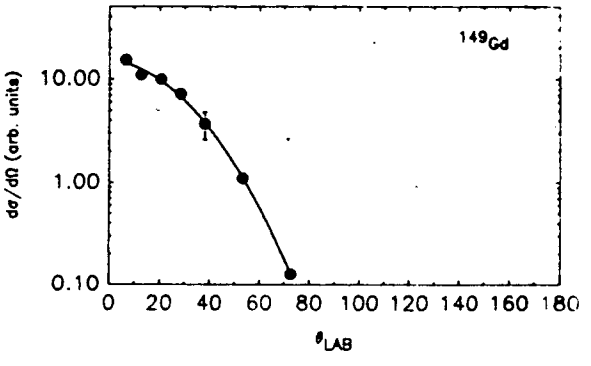
^{149}Gd
dσ/dΩ (arb. units)
10.00
1.00
0.10
0 20 40 60 80 100 120 140 160 180
θ_{LAB}

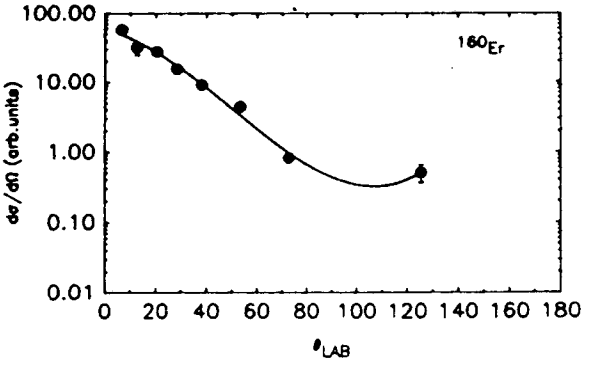
^{160}Er
dσ/dΩ (arb.units)
100.00
10.00
1.00
0.10
0.01
0 20 40 60 80 100 120 140 160 180
θ_{LAB}

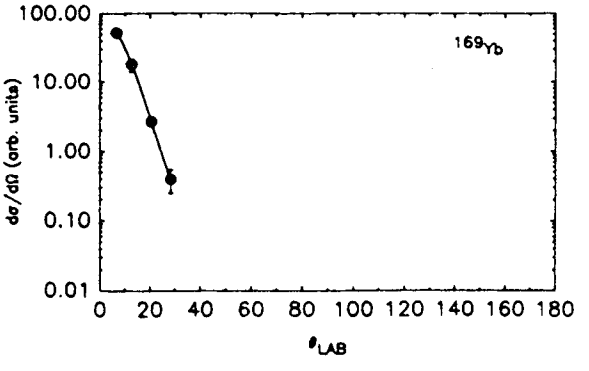
^{169}Yb
dσ/dΩ (arb. units)
100.00
10.00
1.00
0.10
0.01
0 20 40 60 80 100 120 140 160 180
θ_{LAB}

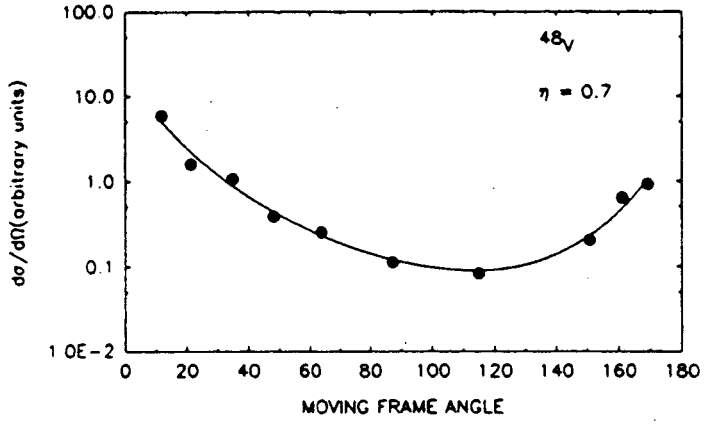
^{48}V
η = 0.7
dσ/dΩ(arbitrary units)
MOVING FRAME ANGLE

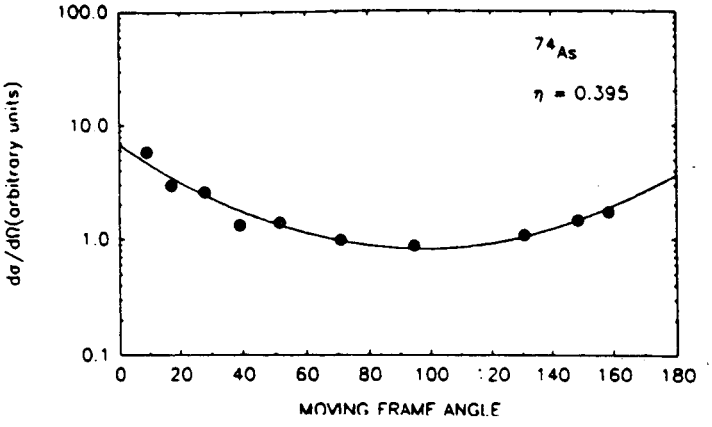
^{74}As
η = 0.395
dσ/dΩ(arbitrary units)
MOVING FRAME ANGLE

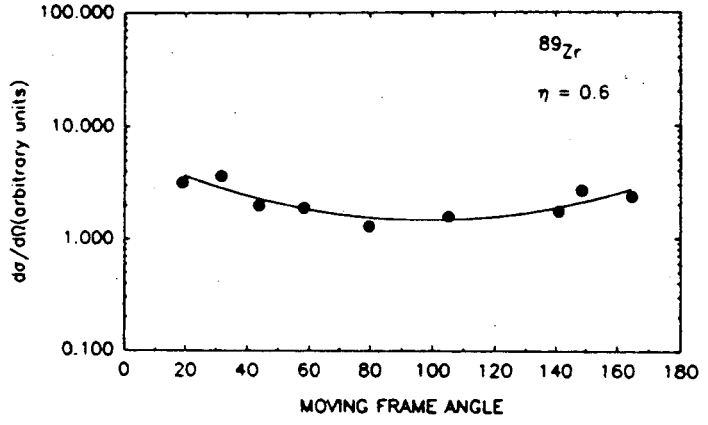
^{89}Zr
η = 0.6
dσ/dΩ(arbitrary units)
MOVING FRAME ANGLE

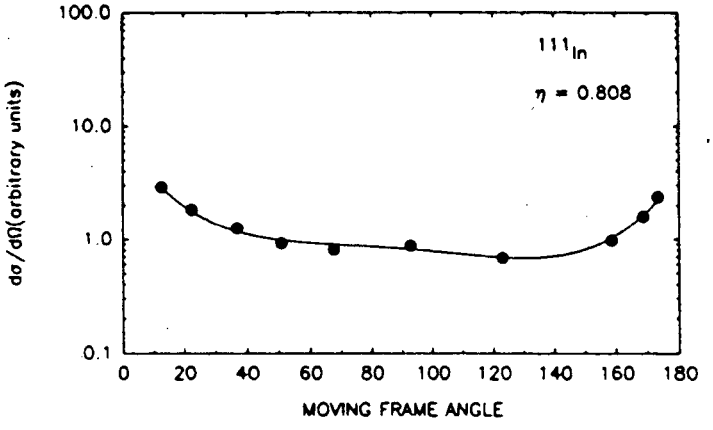
^{111}In
η = 0.808
dσ/dΩ(arbitrary units)
MOVING FRAME ANGLE

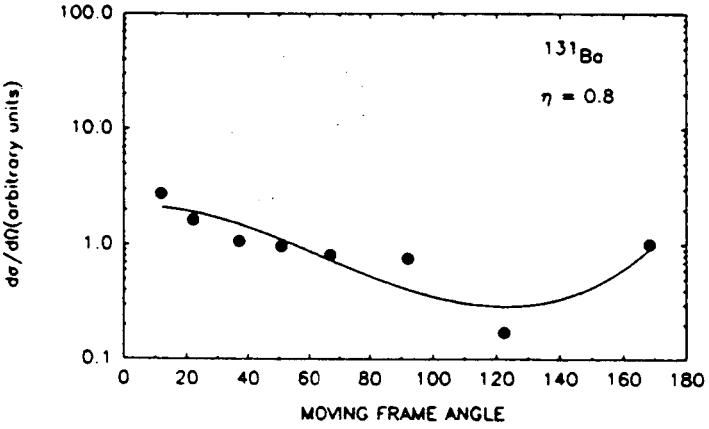
^{131}Ba
η = 0.8
dσ/dΩ(arbitrary units)
MOVING FRAME ANGLE

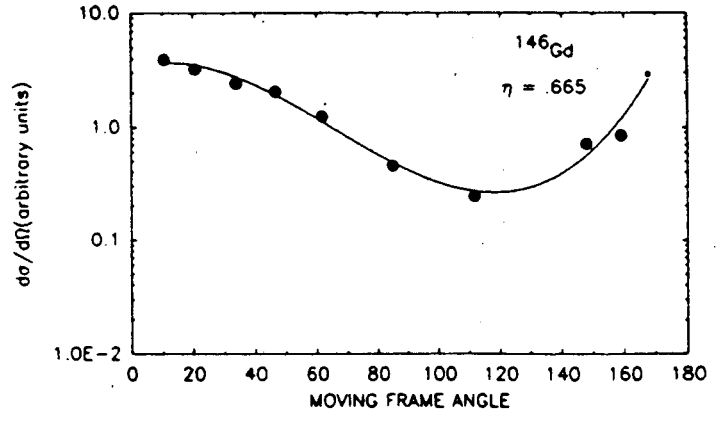
^{146}Gd
η = .665
dσ/dΩ(arbitrary units)
MOVING FRAME ANGLE

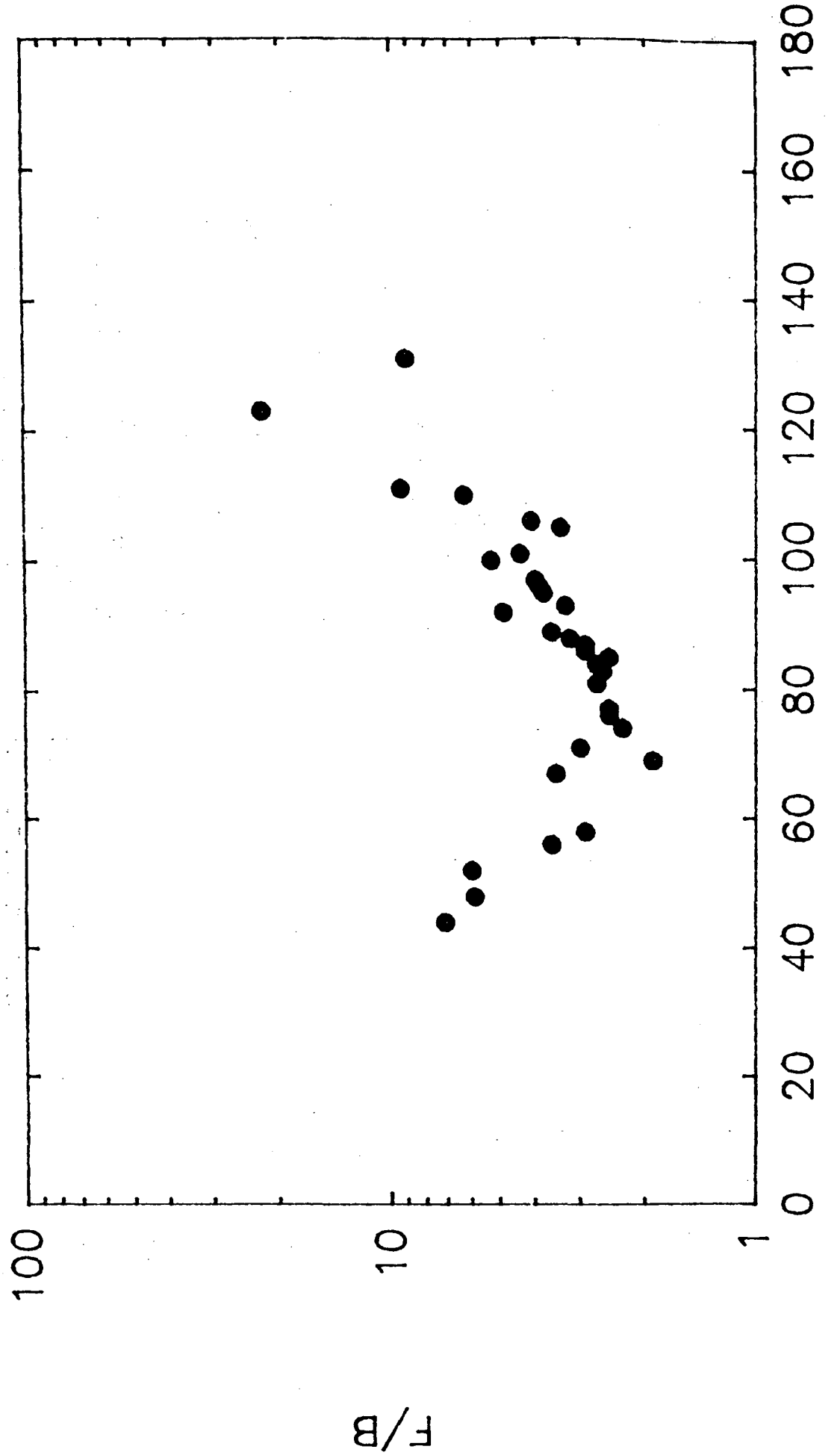
F/B
100
10
1
0
20
40
60
80
100
120
140
160
180
PRODUCT MASS NUMBER A

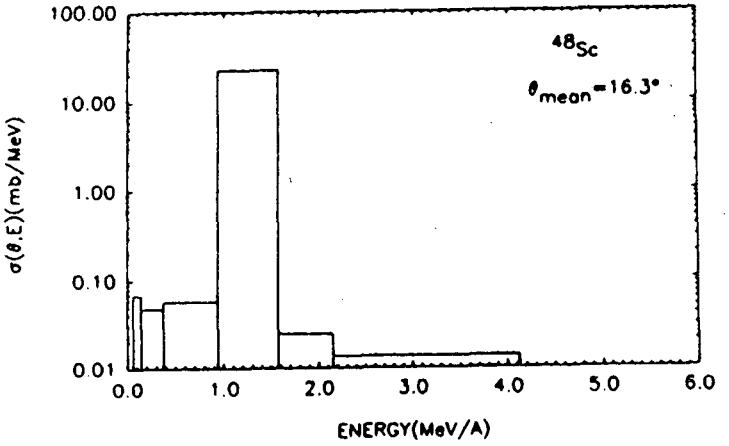
^{48}Sc
θ_{mean}=16.3°
σ(θ,E)(mb/MeV)
ENERGY(MeV/A)

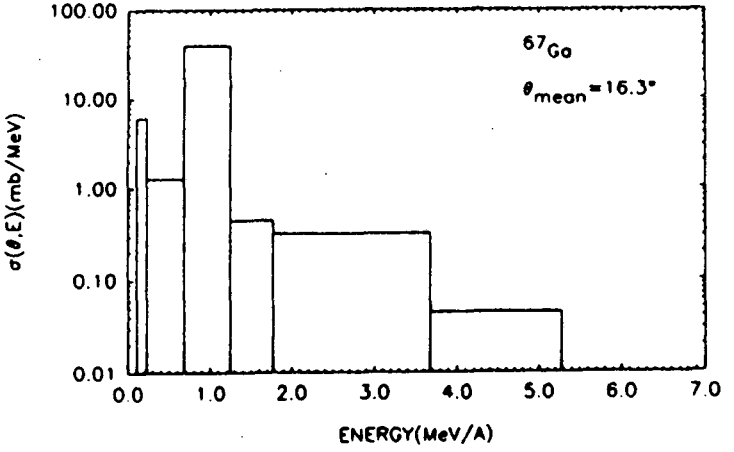
^{67}Ga
θ_{mean}=16.3°
σ(θ,E)(mb/MeV)
ENERGY(MeV/A)

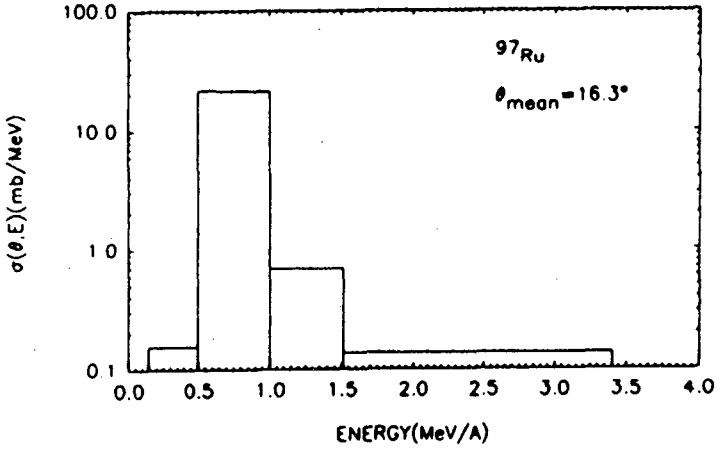
^{97}Ru
θ_{mean}=16.3°
σ(θ,E)(mb/MeV)
ENERGY(MeV/A)

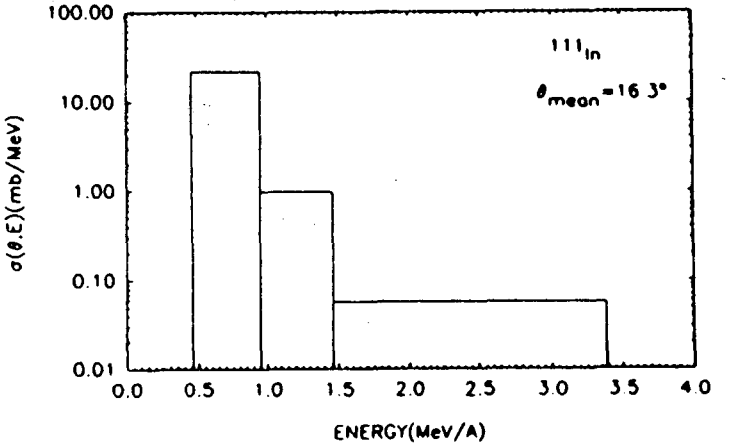
^{111}In
θ_{mean}=16.3°
σ(θ,E)(mb/MeV)
ENERGY(MeV/A)

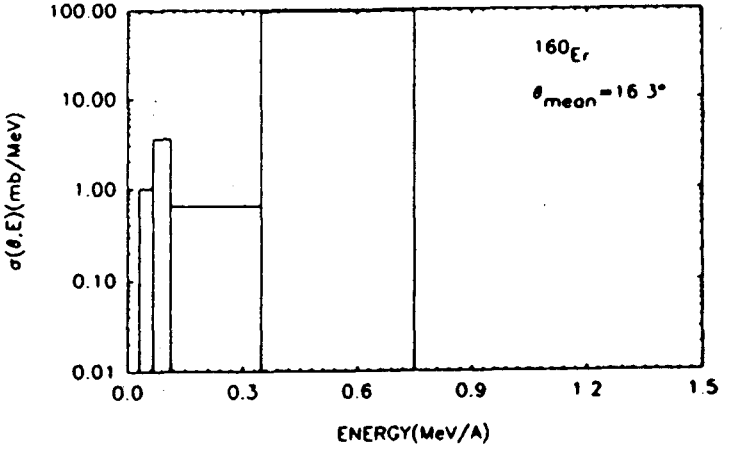
^{160}Er
θ_{mean}=16.3°
σ(θ,E)(mb/MeV)
ENERGY(MeV/A)

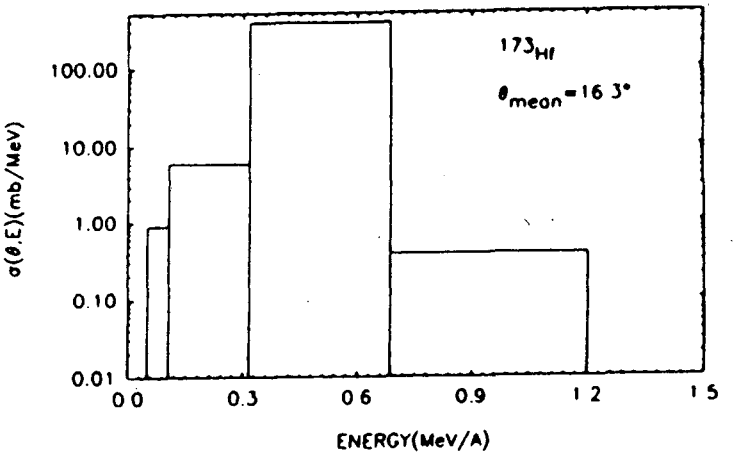
^{173}Hf
θ_{mean}=16.3°
σ(θ,E)(mb/MeV)
ENERGY(MeV/A)

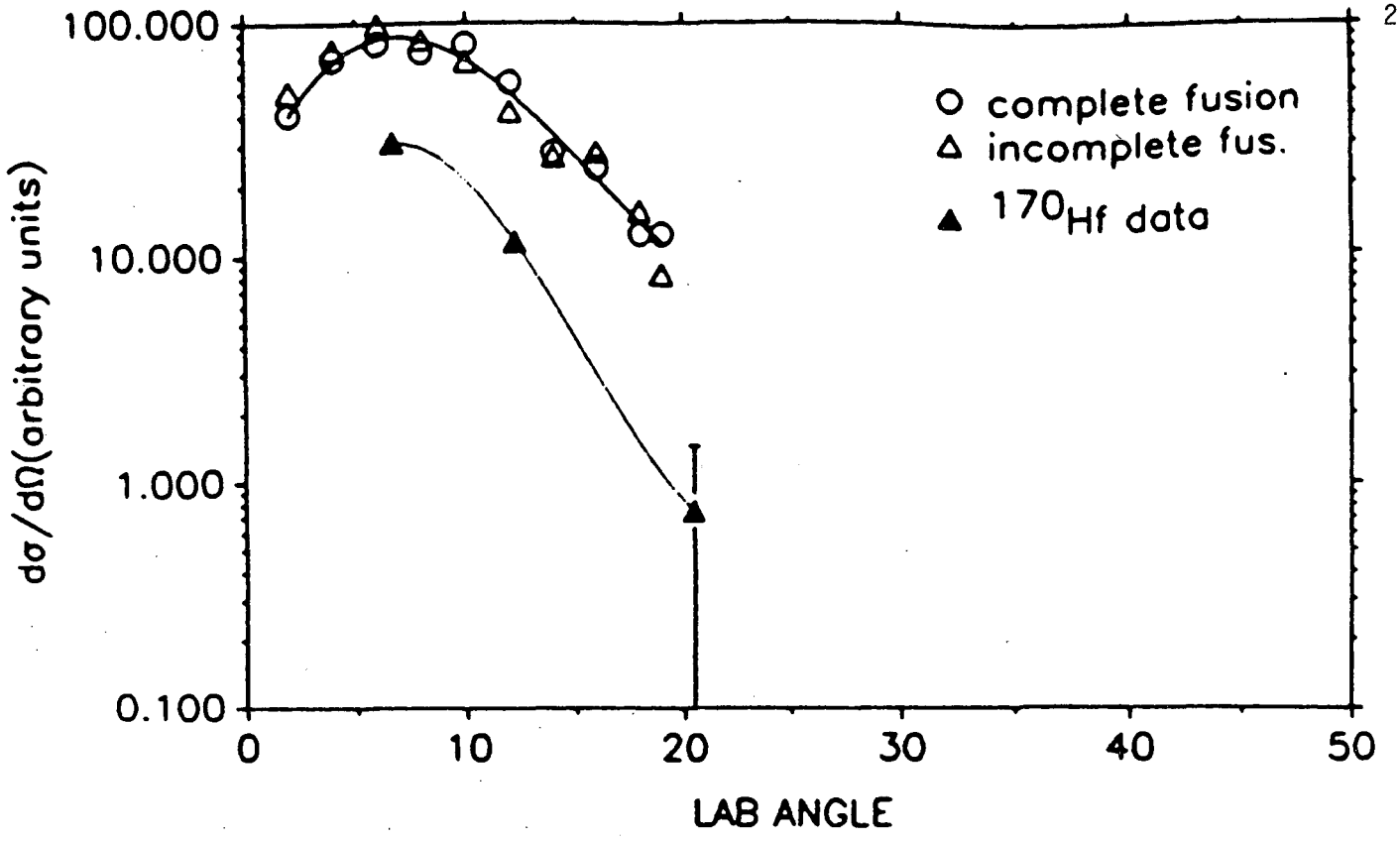
100.000
10.000
1.000
0.100
dσ/dΩ(arbitrary units)
0
10
20
30
40
50
LAB ANGLE
complete fusion
incomplete fus.
170Hf data

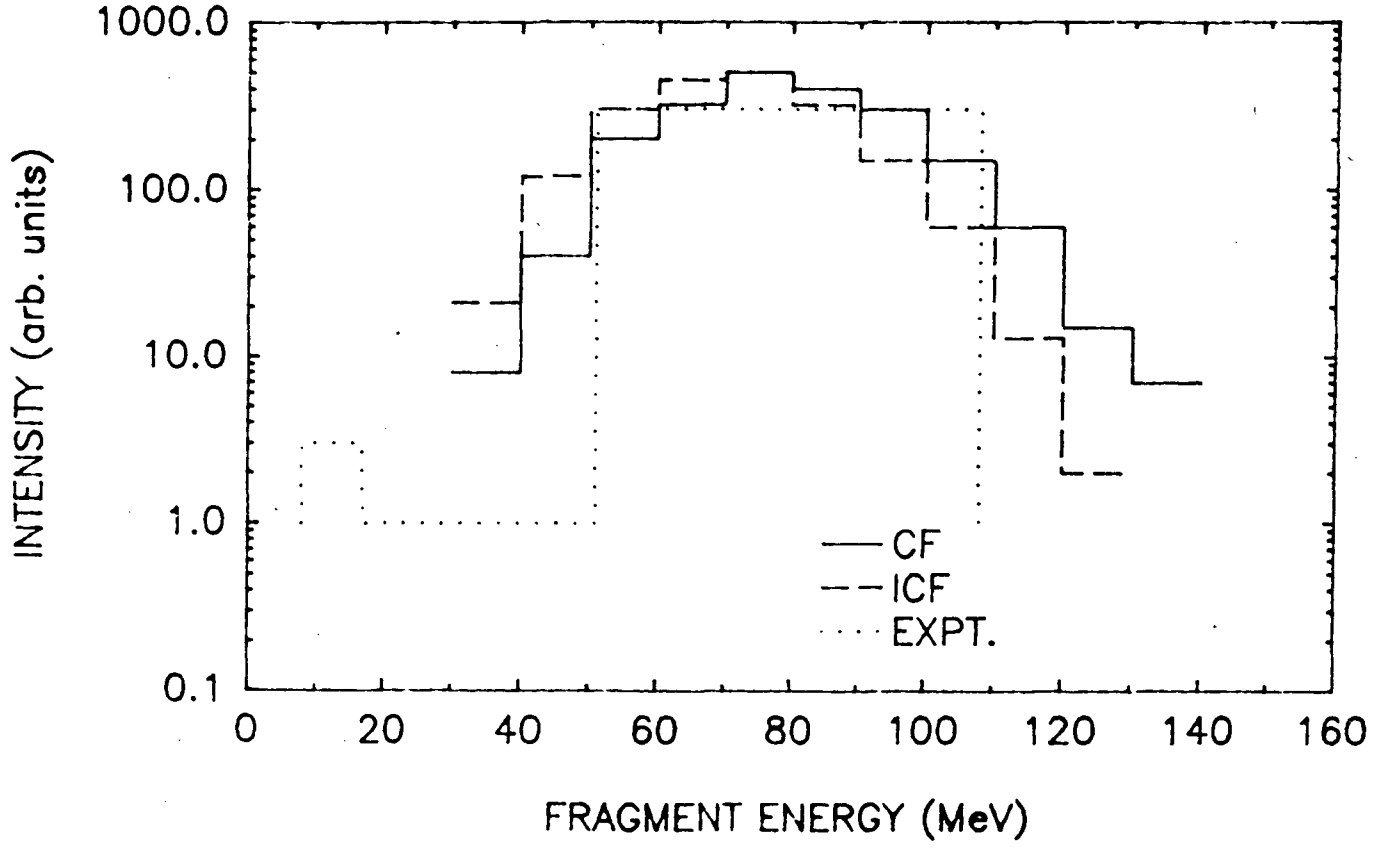
1000.0
100.0
10.0
1.0
0.1
INTENSITY (arb. units)
0
20
40
60
80
100
120
140
160
FRAGMENT ENERGY (MeV)
CF
ICF
EXPT.

LAWRENCE BERKELEY LABORATORY
TECHNICAL INFORMATION DEPARTMENT
UNIVERSITY OF CALIFORNIA
BERKELEY, CALIFORNIA 94720